Electrochemical analysis of the effect of copper tailings on mortars

C. Sepúlveda-Vásquez[a,*], N. Carrasco-Astudillo[b], L. Muñoz[c], C. Guerra[d], and M. Sancy[b,e,f,*]

[a]Departamento de Ingeniería Mecánica y Metalúrgica, Facultad de Ingeniería, Pontificia Universidad Católica de Chile, Santiago, 7820436, Chile.

[b]Escuela de Construcción Civil, Facultad de Ingeniería, Pontificia Universidad Católica de Chile, Santiago, 7820436, Chile.

[c]Instituto de Química, Facultad de Ciencias, Pontificia Universidad Católica de Valparaíso, Valparaíso, Chile.

[d]Faculty of Engineering, University of Nottingham, Nottingham, NG7 2RD, UK

[e]Center for Research in Nanotechnology and Advanced Materials, Pontificia Universidad Católica de Chile, Pontificia Universidad Católica de Chile, Santiago, 7820436, Chile.

[f]Millennium Institute in Green Ammonia, Pontificia, Universidad Católica de Chile, Santiago, 7820436, Chile.

Corresponding authors: Mamié Sancy, Dr. | Carlos Sepúlveda-Vásquez

Escuela de Construcción Civil, Facultad de Ingeniería, Pontificia Universidad Católica de Chile

Santiago, 7820436, Chile

Tel: +56 2 23547908 | e-mail: mamiesancy@gmail.com | cdsepulveda@uc.cl

The research is financed by: ANID PFCHA/Doctorado Beca Chile/2019 (Grant 21190220)

Abstract

The motivation of this study is to promote sustainability in the construction and mining industries from a research perspective, considering the CO_2 emissions associated with cement production and the use of mining waste materials, such as copper tailings, as supplementary cementitious materials. In this study, copper tailings partially replaced cement as received between 0 to 50 wt.%. Mortar and reinforced mortar samples were manufactured for mechanical and corrosion analysis. The mechanical tests revealed that the maximum compressive and flexion strengths were maintained by adding copper tailings, which were delayed for a longer exposure time, possibly due to the hydration reaction. Morphological analysis revealed that the partial cement replacement increased the porosity in the mortar at earlier stages, which was similar for longer exposure time. In addition, electrochemical impedance spectroscopy allowed in-situ monitoring of the mortar's evolution and mortar/steel interface. The impedance response showed that partial cement replacement with 15

wt. % of copper tailings as received can improve steel passivation after prolonged exposure. Therefore, cement replacements can be a suitable solution to produce reinforced mortars.

Keywords: copper tailing, supplementary cementitious material, electrochemical behavior, mechanical properties.

1. Introduction

Concrete is one of the most used materials worldwide in the construction industry, involving the production of more than 4 billion tons of cement annually (Cao et al., 2016; Mehenni et al., 2016), also generating about 8 % of global carbon dioxide (CO2) emissions (Kajaste & Hurme, 2016). It has been reported that 1 ton of cement produced releases between 0.73 and 0.99 tons of CO_2 (Lehne & Preston, 2018; Pacheco Torgal et al., 2012). Cement is mainly composed of Portland clinker, the production of which accounts for more than 50 % of the emissions associated with the limestone calcination process ($CaCO_3$) (Cao et al., 2016; Hasanbeigi et al., 2012a; Medina et al., 2020) that is carried out at temperatures ranging from 1400-1600 °C (Imbabi et al., 2012). One of the alternatives is the substitution of clinker for supplementary cementitious materials (SCM), allowing for reducing the emissions associated with the calcination process (Hasanbeigi et al., 2012b; Petersson et al., 2008).

SCMs correspond to soluble powders composed mainly of silica (Juenger et al., 2019; Juenger & Siddique, 2015), which, depending on their origin, can be assigned an energy cost. For example, kaolinite clays require a thermal energy equal to 0.35 GJ/t to transform into a SCM, corresponding to 10 % of the thermal energy needed to generate clinker. While industrial wastes have a lower energy than clinker production (Hossain et al., 2018), since their output has no associated costs, they also have potential technological opportunities when finding an application. It has been reported that the use of SCM contributes to the cementitious matrix in two ways: (1) chemical due to the reactions of the hydration products of portlandite and aluminosilicates, generating second-order hydrated calcium silicates (CHS), known as pozzolanic effect; and (2) physical associated with the interaction between the particles and the surface in the hydration products, known as filler effect (Vargas & Lopez, 2018). Therefore, SCM can improve the mechanical behavior and durability of concrete. Güneyisi et al. (Güneyisi et al., 2012) reported that the addition of metakaolin between 5 - 15 wt. % to concrete increased its compressive strength by close to 40 % after 28 days, which was attributed to the better bond between the cement paste and the aggregate due to the quality of the cement paste. In addition, the authors determined an increase in the durability of concrete due to the surface absorption of water by the decrease in porosity generated by a dense production of C-H-S (Juenger & Siddique, 2015).

To reduce the carbon footprint and promote green and environmentally friendly construction, mining industry waste has been proposed as SCM, such as copper tailings composed of silicon, alumina, and iron (II) oxides, which are also readily available. Some studies have evaluated mortar and concrete mechanical properties with different copper tailing replacements. For instance, Onuaguluchi and Eren (Onuaguluchi & Eren, 2012b) reported that by replacing 10 % of the cement mass with copper tailings, the compressive strength of concrete increased by 16.2 % after

28 days and increased the sulfate expansion potential. Vargas and López (Vargas & Lopez, 2018) studied copper tailings from different mines in Chile, concluding that the origin of the tailings influences the mechanical behavior in mortar samples, determining a decrease in the compressive strength with 20 wt. % cement replacement. Dandautiya and Singh (Dandautiya & Singh, 2019) studied the combined use of fly ash and copper tailings, finding that the most favorable mix was with 20 wt. % replacement of cement by fly ash and 5 wt. % by copper tailings, increasing the compressive strengths concerning the sample without replacement by 8.27 %. The authors also reported a 14 % reduction in CO_2 equivalent release for replacing 10 % fly ash and 5 % copper tailings. Esmaeili et al. (Esmaeili et al., 2020; Esmaeili & Aslani, 2019a) studied the replacement of copper tailings from mines in Iran, finding that the compressive strength improved with cement replacement up to 30 % at 90-day ages, which they associated with pozzolanic and filler effect and slow hydration process, determining that the optimum cement replacement varied between 15- 20 wt. %.

Few studies focus on how the copper tailing can affect the reinforced bars embedded in mortar. For example, Abd et al. investigated corrosion mitigation in reinforced concrete in the Arabian Gulf, observing corrosion mitigation using fly ash and slag cement as SCM. The authors determined corrosion current densities (I_{corr}) close to 0.25 μA/cm^2, which was around 2.20 μA/cm^2 for ordinary Portland cement (OPC) (Abd et al., 2018). Koga et al. studied the effect of added fly ash through open circuit potential (Eoc) measurements, which shifted towards slightly more positive values in the samples with fly ash, reaching similar I_{corr} values after 365 days (Koga et al., 2018). Montemor et al. observed an increase in load transfer resistance with fly ash content for the replacement of 30 wt. % fly ash, an increase that was by a 4-5 factor for samples without replacement, which was mainly associated with pozzolanic reaction due to the reduction of porosity and increasing the resistivity of the mortar (Montemor et al., 2000). Zhang et al. investigated concrete samples with copper tailings replacements, observing the formation of crystals in the concrete pores and obtaining compact concrete with 20 wt.% of cement replacement. However, with 30 wt. % of copper tailings, the formation of crystals destroyed the structure around the concrete pore, suggesting that the density of the concrete matrix determines the corrosion resistance due to the filler and pozzolanic effect of the SCMs materials (Zhang et al., 2019). Furthermore, Zhao et al. investigated the impact of iron-copper tailings on the mechanics and durability of steam-cured mortars (Zhao et al., 2023). The authors determined an increase in the compressive strength by 1.09% and 7.27% using 10 wt.% of cement replacement after 1 and 28 days, reporting a reduction in the permeability with 10 wt.% to 20 wt.% of iron-copper tailing. Therefore, the researcher proposed that a higher substitution level is not beneficial for durability because SCM can increase the conductivity compared to reference samples. Wang et at. (Wang et al., 2023) analyzed the effect of tannic acid (TA) on the reactivity of copper tailings as SCM, determining that the TA-functionalized copper tailings promoted long-term hydration in mortars and densified the interfacial transition zone between the copper tailings and hydration products, decreasing the porosity. The average compressive strength increased by 35.6% at 28 days. Onuaguluchi and Eren added copper tailings as SCM on mortars´ fresh and hardened, between 0 % to 10 wt.%. The dry copper tailings negatively affected the mixture, which was improved using pre-wetted copper tailings. Thus, the copper tailings blended mortars improved the compressive strength and abrasion resistance. Additionally, the acid and

chloride resistance increased compared to the control mixture (Onuaguluchi & Eren, 2012a).

Therefore, this work focused on the fundamental understanding of the effect of adding copper tailings as SCM in mortars and metallic bars, studying their morphological, microstructural, mechanical, and electrochemical responses at different exposure times.

2. Methodology

2.1 Copper tailing characterization

The chemical composition of the tailings was determined by Energy-Dispersive X-ray Spectroscopy (EDS) using a FE-SEM Model QUANTA 250 FEG. Copper tailing powders were also analyzed by X-ray fluorescence using Oxford Instruments Handheld XRF - X-MET7500, equipped with Two-Beam Mining and Soil 3 Beam. All samples were analyzed in triplicate. Microstructural analysis of the copper tailings was performed using X-ray diffraction (XRD) with a Bruker D8 Advance diffractometer of 40 kV and Rigaku with a Cu $K_{\alpha 1,2}$; K_{β} source. The diffractograms were recorded between angles $2\theta = 10° – 80°$, using a scan rate of 0.02 $°\cdot s^{-1}$ at room temperature.

2.2 Sample fabrication

Mortar mixtures were manufactured with Portland cement replacement according to the ASTM C 595: Type P (Portland-Pozzolanic Cement) standard, using copper tailings as partial cement replacement, between 0-50 wt. %. The water/cement (w/c) ratio was 0.65, slightly higher than that often used to understand the copper tailing addition's effect on the corrosion properties of reinforced mortars.

Prismatic mortar samples were manufactured to be mechanically tested according to ASTM C305, as shown in Figure 1(a). Reinforced mortar samples were fabricated for corrosion analysis using striated A630 carbon steel bars, 150 mm long and 8 mm in diameter. The A630 bars were cleaned through chemical pickling (3 times), drizzled with an anhydrous ethanol solution, and dried with warm air in agreement with ASTM G1. Then, steel bars were painted with anticorrosive paint to isolate a specific area and later embedded in a mortar mix after 24 h, as shown in Figure 1 (b). All samples were manufactured in triplicate.

2.2.1 Exposure

Mortar and reinforced mortar samples were exposed to a saturated solution $Ca(OH)_2$ at 23 °C.

2.4 Mechanical evaluation

Compressive strength and flexural tests were performed on the prismatic samples after 7, 14, and 21 days of exposure to a saturated solution $Ca(OH)_2$, according to standard ASTM C109 standard. Figure 1 shows a schematic draw and digital image of the samples used for the mechanical characterization. All samples were analyzed in triplicate.

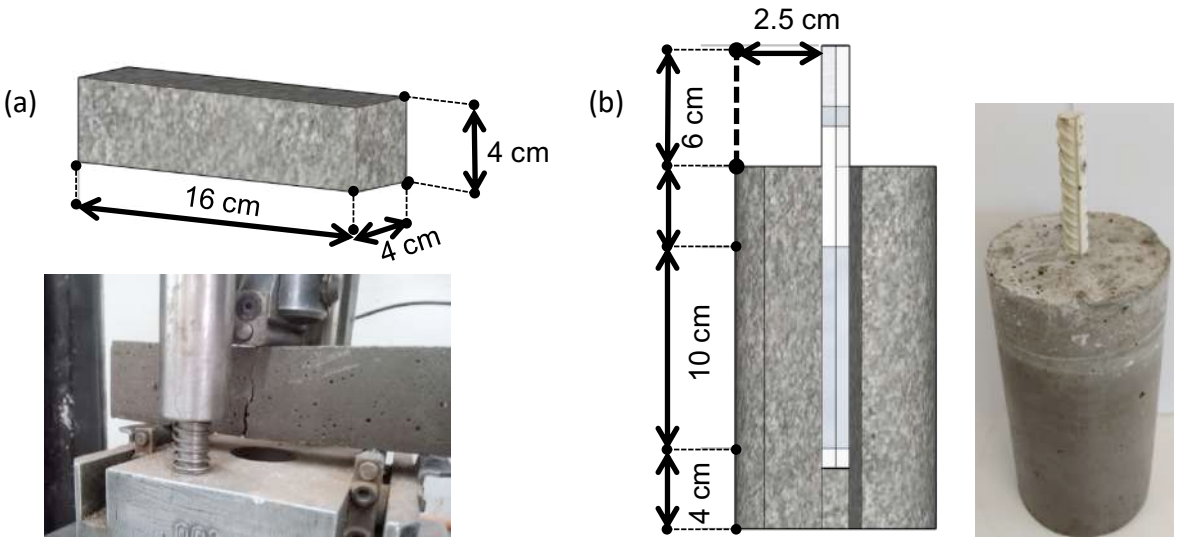

Figure 1. Images and scheme representation of samples for (a) mechanical tests and (b) electrochemical measurements. The gray color in the steel bar (b) represents the non-coated part in the metal sample.

2.5 Electrochemical evaluation

The electrochemical tests were measured using a potentiostat/galvanostat (Bio-Logic, VSP), a three-electrode electrochemical cell, with graphite and a saturated calomel electrode (SCE) employed as the counter and reference electrodes, respectively. Reinforced mortar was used as the working electrode, with a geometrical exposure area of 25.13 cm^2. Open circuit potential (E_{OC}) and electrochemical impedance spectroscopy (EIS) measurements were collected after 7, 21, 28, and 56 days of exposure. EIS measurements were carried out between 65 kHz to 3 mHz, with seven points per decade, using a ±10 mV peak-to-peak sinusoidal voltage at $E = E_{OC}$. The EIS data were fitted using SIMAD (LISE UPR 15 CNRS, France). Additionally, EIS was performed at $E = E_{OC} \pm 200$ mV vs. SCE after 120 days of exposure.

2.6 Morphological characterization

A scanning electron microscopy (SEM) Hitachi SU3500 model was used to characterize the copper tailings and mortar surfaces before and after exposure.

3. Results and discussion

3.1 Copper tailing characterization

Figure 2(a,b) shows the morphology of copper tailings as received, revealing irregular shapes, with a log-normal distribution particle size distribution (PSD), which ranged between 0.1 µm to 400 µm, passing 50 % at 110 µm and 90 % at 400 µm. It should be noted that the particle size in Portland cement has 90 % of particles around 50 µm Several studies have demonstrated that tiny particles of SCM favor the cement hydration kinetic pozzolanic reaction rate and strength gain, which can be related to an increase in the mixture viscosity, reducing the potential of mixture workability (Ayati et al., 2022; Sun et al., 2022).

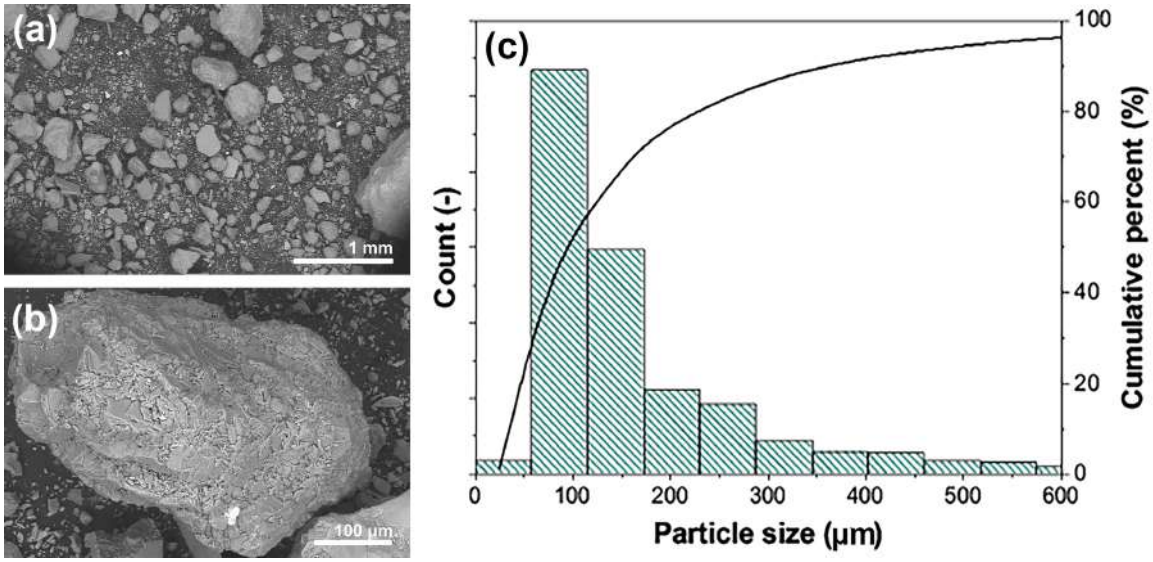

Figure 2. (a,b) SEM images of copper tailing and (c) particle distribution processes by IMAG J from SEM images.

Researchers have proposed that the particle number density and the interparticle force are the most critical parameters that impact the mix's viscosity (Navarrete et al., 2022). Bentz et al. (Bentz et al., n.d.) studied the cement PSD through computer simulation and experimentally, reporting that the coarser particle size offers superior hydration. Nevertheless, it has also been proposed that small particle size reduced the

permeability and attack of concrete sulfates, segregation, mechanical resistance, and durability. The effect was associated with the pozzolanic activity in ordinary Portland cement, which can react with the Portlandite ($Ca(OH)_2$) present in the cement paste, generating hydrated calcium silicates (C-H-S) of second order (Pacheco Torgal et al., 2012).

Table 1 shows the chemical composition of copper tailing as received, obtained by EDS and XRF, revealing that Si, Ca, S, and Al were the main chemical elements (in wt.% from EDS analysis). In addition, Table 1 shows that Fe, S, K, Ca, Cu, Pb, Cd, and As were in a concentration (in mg/kg) below the permissible values by the standards Standard 503 - 40 CFR/1993 (US EPA, 1993) and Australian Standard AS 4454-1999 (ANZANZEC, 2000). Therefore, copper tailing does not present harmful amounts for use as SCM.

Table 1. Chemical composition analysis of copper tailing obtained from EDS and XRF analyses.

Element	Si	Al	Fe	S	K	Ca	As	Cd	Pb	Cu	Hg
EDS (wt.%)	46.0	12.3	1.4	13.9	10.0	16.4	-	-	-	-	-
XRF (mg/kg)	-	-	5688	1738	26,333	11,244	5.6	10.3	10.7	397	3.2

Figure 3 shows the XRD patterns of copper tailing as received, which reveals the presence of Albite $(Na,Ca)Al(Si,Al)_3O_8$), α-quartz (α-SiO_2), Sanidine ($KAlSi_3O_8$), calcium silicates, as also reported by Qing (Mabroum et al., 2020; Qing et al., 2021). It should be mentioned that OPC comprises Portlandite, Ettringite, calcite, and α-quartz (Medina et al., 2020). The quantitative analysis using EVA software revealed that 57.3 wt.% corresponds to Albite, 30.7 wt.% to α-quartz, 9.1 wt.% corresponds to Sanidine, and 2.9 wt.% to calcium silicates. It has been reported that Albite and Sanidine can have a pozzolanic activity (Lothenbach et al., 2017)(Pokorný et al., 2016).

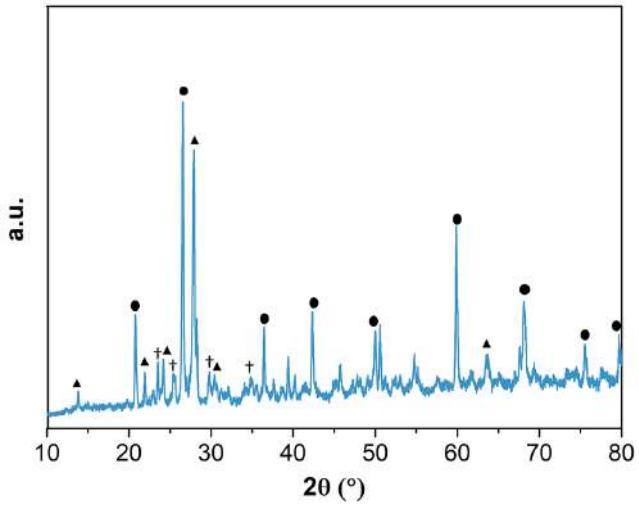

Figure 3. X-ray pattern of copper tailing. (▲) Albite ((Na,Ca)Al(Si,Al)$_3$O$_8$) (Ca$_2$(SiO$_4$), (†) Sanidine (KAlSi$_3$O$_8$), (•) quartz (α-SiO$_2$,quartz-low).

3.2 Morphological and mechanical mortars analysis

Figure 4 shows the maximum compression strength and flexion as a function of exposure and cement replacement. For all samples, the mechanical properties increased over time but slowed for cement replacement greater than 20 wt.%. It should be noted that the maximum compressive strength was similar between the control samples and cement replacement with 15 wt.% and 20 wt.% after 7 and 14 days of exposure. However, the maximum compressive strength increased more drastically for the control sample for a longer exposure time, possibly due to a delay in the hydration reaction. The flexion strength shows a similar response to the compressive strength. It should be noticed that similar behavior for cement replacement using copper tailing has been studied (Esmaeili & Aslani, 2019b; Zhang et al., 2019). Vargas et al. (Vargas et al., 2020) reported a more significant delay using a w/c ratio greater than 0.5, demonstrating that the mechanical properties can be improved by adding more than 20 wt. % copper tailings thermally pre-treatment and milled. A similar phenomenon has been observed using over 30 wt. % cement replacement of fly ash (Sánchez de Rojas et al., 2008). It has been reported that a high crystallinity of the SCM (Smuda et al., 2008, 2014) does not allow a pozzolanic effect in the cement matrix (Onuaguluchi & Eren, 2012b; Vargas & Lopez, 2018). In this context, Zhang et al. (Zhang et al., 2019) proposed that mechanical behavior close to the control samples can be achieved using 15 wt. % cement replacement. However, the dissolution of the cement paste limits the mechanism with a more significant amount of SCM.

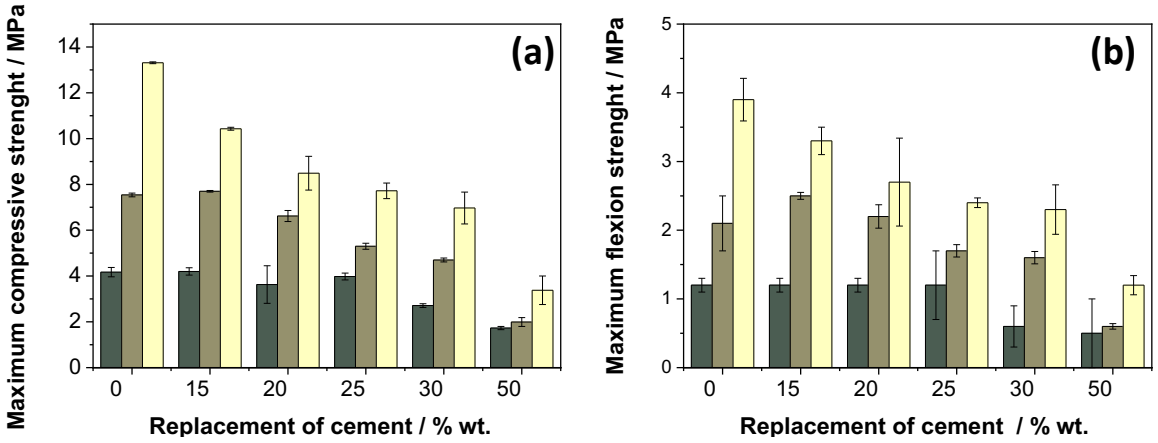

Figure 4. Mechanical properties of mortars with different cement replacement percentages after exposure to saturated $Ca(OH)_2$ solution. (a) maximum compressive strength, and (b) maximum flexion. (■) 7 days, (■) 14 days, and (■) 21 days.

Figure 5 shows SEM images of mortar samples with different cement replacements after short (14 days) and long (120 days) exposure time in a saturated $Ca(OH)_2$ solution, revealing an increase in the porosity and a reduction in the density with the cement replacement after short exposure time. For instance, samples with 20 and 30 wt. % of cement replacement have lower densities and more extensive pore distribution than the control samples, which is consistent with the previous mechanical results. However, all samples have a similar density for long exposure time. Therefore, the increase in the cement replacement by copper tailing can reduce the pozzolanic activity at an early stage. Nevertheless, this can be improved for a longer exposure time.

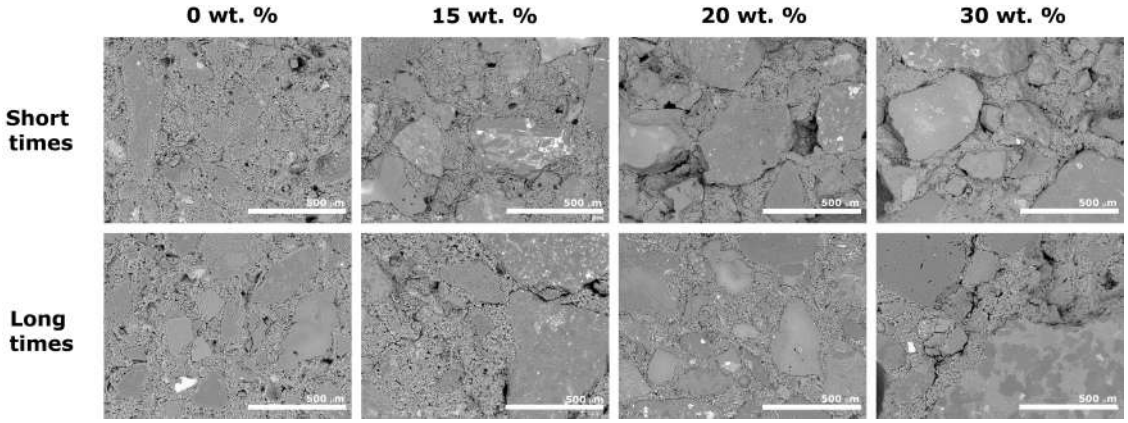

Figure 5. SEM images of mortars with different cement replacement percentages after 14 and 130 days to saturated $Ca(OH)_2$ solution.

3.3 Electrochemical behavior of reinforced mortars

Figure 6 shows the evolution of the open circuit potential (E_{oc}) of reinforced mortar samples after exposure time, with different percentages of cement replacement, revealing that the E_{oc} values were close to -250 mV vs. SCE for samples with 0, 20, 25, and 30 wt.% as cement replacement, which, according to ASTM C876, are not under a corrosion probability (ASTM International, 2015). The E_{oc} value varied from -300 to -200 mV vs. SCE for samples with 15 wt.% as cement replacement, suggesting a possible improvement in the protection of the steel bar. The sample with 50 wt. % replacement showed more negative E_{oc} values. Stefanoni et al. (Stefanoni et al., 2018) proposed that the more negative potentials of the metallic bar embedded in carbonated concrete were associated with a high corrosion rate. Hemkemeier et al. (Hemkemeier et al., 2022) also reported a shift in the E_{oc} values using industrial wastes in cementitious composites. The authors proposed that using wastes is beneficial to short exposure time rather than longer exposure time for the steel bar. The authors suggested two origins: (i) An increase in porosity due to the waste incorporation could facilitate the exchange of ions. (ii) The releasing ions by the cementitious supplementary materials could influence the metal bar corrosion.

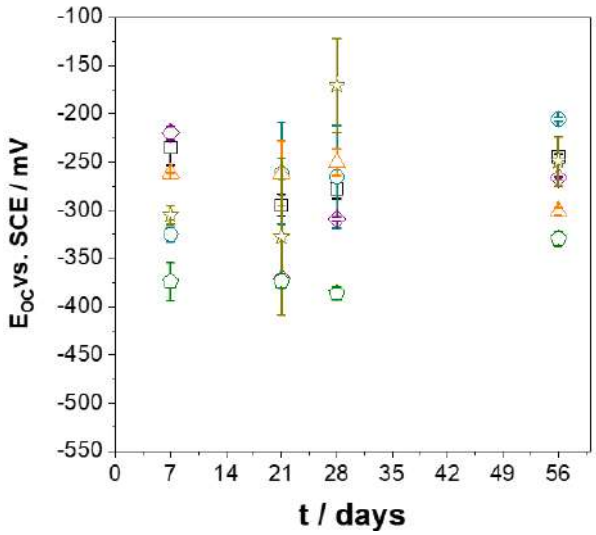

Figure 6. Effect of copper tailing addition on the open circuit potential of reinforced mortar samples after exposure to saturated $Ca(OH)_2$ solution at 23 °C.
(□) 0 wt. %, (○) 15 wt. %, (△) 20 wt. %, (◇) 25 wt. %, (☆) 30 wt. % & (⬟) wt. 50%.

Figure 7 shows the Nyquist diagrams of reinforced mortar samples with 15 wt. % cement replacement after 120 days at different over-potentials. Nyquist diagrams show two capacitive loops, both incompletes, at very high (VHF) and at medium and low

frequency (MF-LF). The capacitive loop at VHF has been previously related to the cementitious part of the reinforced mortar samples, and the capacitive loop at MF-LF has been attributed to the carbon steel dissolution process. Novoa (Nóvoa, 2016) attributed the impedance response at VHF to several factors, such as porosity, pore size distribution, and dielectric properties of cementitious cover. The impedance responses at different overpotentials do not reveal a significant effect between them. This suggests that the anodic and cathodic reactions are in a mixed control, having similar contributions to the mechanism.

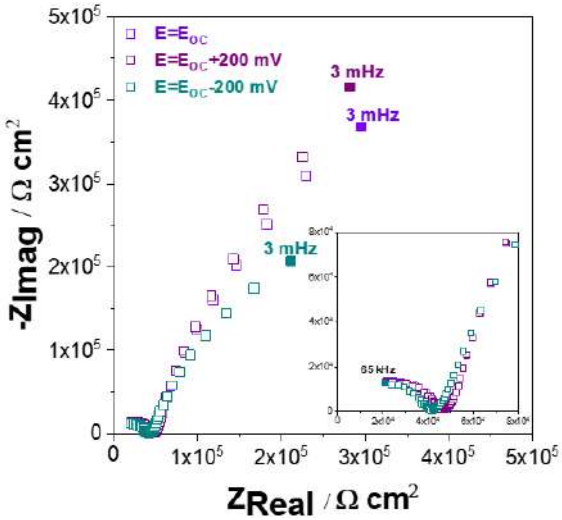

Figure 7. Effect of over-potential on the impedance response of reinforced mortar samples with 15 wt. % of cement replacement after 120 days of exposure to saturated $Ca(OH)_2$ solution at 23 °C.

Figure 8 shows the Nyquist diagram of reinforced mortar with a 15 wt. % cement replacement over time. The impedance data were adjusted and simulated using the equivalent circuit shown in Figure 9, based on the previous equivalent circuit at VHF proposed by Novoa (Novoa, 2016). Figure 8 reveals that the impedance response at VHF was drastically influenced by the exposure (see inset image), suggesting an increase in the cementitious matrix resistance due to incorporating the copper tailing as SCM. This can be associated with the evolution of hydration processes, which continue during exposure. However, the impedance response at MF-LF was not significantly affected, possibly due to the passivity of the carbon steel.

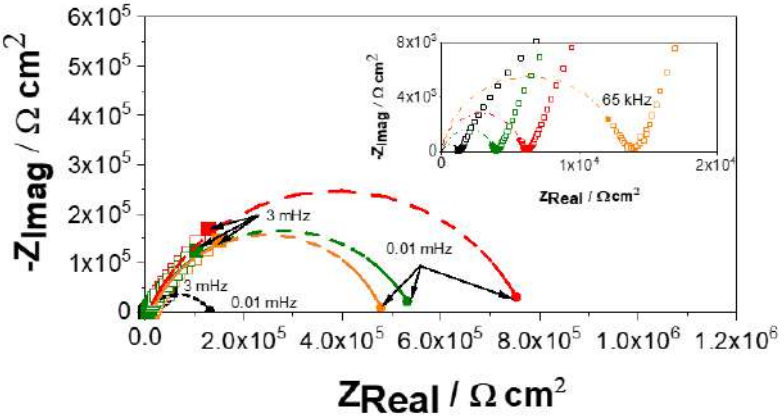

Figure 8. Nyquist diagrams of the reinforced mortar with 15 wt. % after exposure to saturated $Ca(OH)_2$ solution at 23 °C and $E=E_{oc}$. (□) 7, (□) 21, (□) 28, and 56 days (□).

Figure 9 shows that percolating pores correspond to the interconnected porosity, and occluded pores are related to the insulated pores in the physical model. The equivalent circuit proposed for reinforced mortar included non-ideal capacitances for the bulk part and occluded pores. Several authors have proposed a frequency distribution on the impedance (Gharbi et al., 2019; Jorcin et al., 2006) (Z) that can be expressed by a constant phase element (CPE), whose parameters are Q and α. In the equivalent circuit, R_P represents the percolating pore resistance, R_{OP} corresponds to the occluded pore resistance, CPE_{bulk} represents the capacitance of the solid phase in the mortar, and $CPE_{occluded}$ represents the capacitance of close porosity that is not interconnected. R represents a resistance composed of the oxide layer resistance and charge transfer resistance, and CPE represents a pseudo-capacitive composed of the electrical double layer and oxide layer. The morphological changes were attributed to the evolution of the hydration process related to changes in porosity and conductivity, as described by Andrade et al. (Andrade et al., 2001).

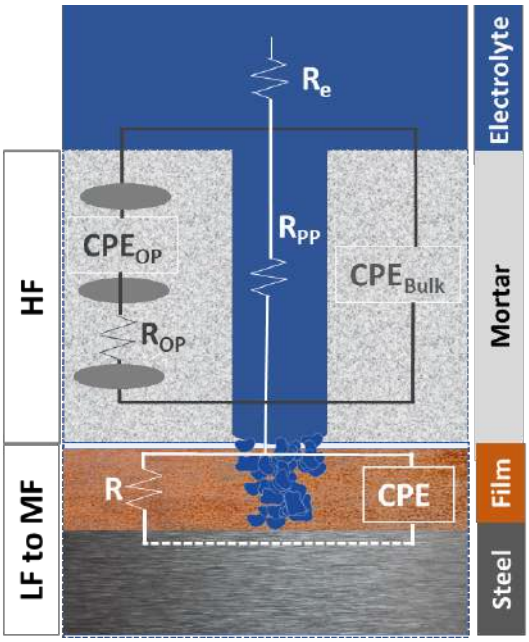

Figure 9: Equivalent circuits used for impedance data of reinforced mortars exposed to saturated $Ca(OH)_2$ solution at $E = E_{OC}$

Figure S1 shows a summary of CPE parameters attributed to the bulk part of mortars as a function of exposure time, obtained by adjusting, revealing that the Q_{bulk} was not varied with a clear trend during exposure, reaching values around 10^{-9} – 10^{-10} $F \cdot s^{(\alpha-1)} \cdot cm^{-2}$ for longer exposure time. The Q_{bulk} variability could be associated with the hydration reactions in the bulk part of the reinforced mortars. Note that the control samples were more stable than those with cement replacement, which had lower Q_{bulk} values than the control sample. This can be attributed to a delay in the hydration process in the presence of copper tailing as SCE, possibly due to a higher interconnected porosity density that facilitates electrolyte diffusion and chemical reaction in the mortar, mainly for samples with cement replacement higher than 20 wt. %. Figure S1(b) shows the α_{bulk} variation as a function of cement replacement and exposure, which varied between 0.7 and 0.97, without a clear trend, suggesting that all samples have a similar mechanism independent of cement replacement.

Figure 10 shows the variation of the percolating and occluded pore resistances of reinforced mortar samples after exposure to $Ca(OH)_2$ solution as a function of exposure time obtained by adjusting. Both types of pore resistance increased during exposure, particularly at earlier stages, possibly due to the evolution of the hydration reaction in mortars. It should be noted that for the samples with a 50 wt. % of cement replacement,

R_P decreased was recorded after 21 days. However, R_P increased after 56 days, reaching similar values to other samples with lower cement replacement. This response also suggests that adding copper tailings can cause a delay in the hydration reaction and hardness, as previously discussed. Note that RP progressively increased as the control sample for the sample with a 15 wt. % of cement replacement.

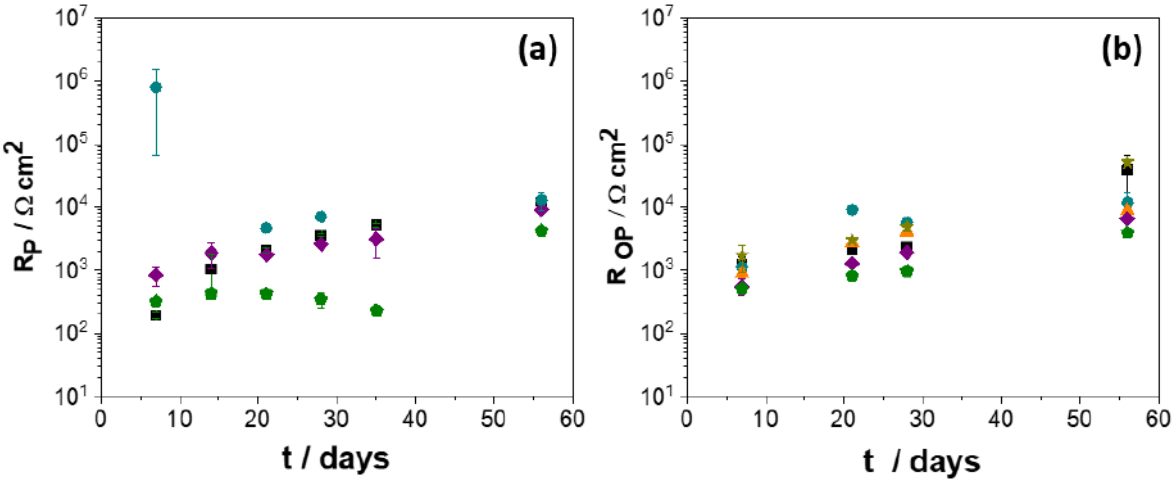

Figure 10: Variation of percolating and occluded pore resistance of reinforcement mortars in $Ca(OH)_{2,sat}$ at 23 °C and E=E_{oc}. (■) 0 wt. %, (●) 15 wt. %, (▲) 20 wt. %, (♦) 25 wt. %, (★) 30 wt. % & (⬟) wt. 50%.

As mentioned above, the impedance response in the MF-LF ranges was related to the mortar–steel interface (Andrade et al., 1995, 2001; Nóvoa, 2016), which was fitted with a simple Randles-type equivalent circuit, where a pure capacitance was replaced by a CPE_{MF-LF}, as proposed by Gonzalez et al. (Gonzalez et al., 1985) and Liu et al. (Liu et al., 2017). Figure 11 shows the variation of CPE parameters (Q_{LF} and α_{LF}) at MF-LF ranges related to the carbon steel dissolution in the cementitious matrix as a function of exposure time. As can be seen, the Q_{LF} value was around 0.7 $x10^{-4}$ and 3 $x10^{-4}$ $F{\cdot}s^{(\alpha-1)}{\cdot}\ cm^{-2}$ after 21 days of exposure, reaching the highest values with 15 wt. % cement replacement and the lowest with 50 wt. % replacement. Figure 11(b) shows the α_{LF} variation over time, revealing a higher variation at earlier stages and reaching more stable values for longer exposure time. This behavior suggests an improvement in the passivation of the carbon steel for all samples, which have a similar behavior to those found by Nanqiao et al. (You et al., 2022). The authors reported similar Q_{LF} values related to a passive layer formed on the steel surface, which was exposed to an alkaline environment. Therefore, the addition of copper tailings does not modify the stability of the passive layer on the steel.

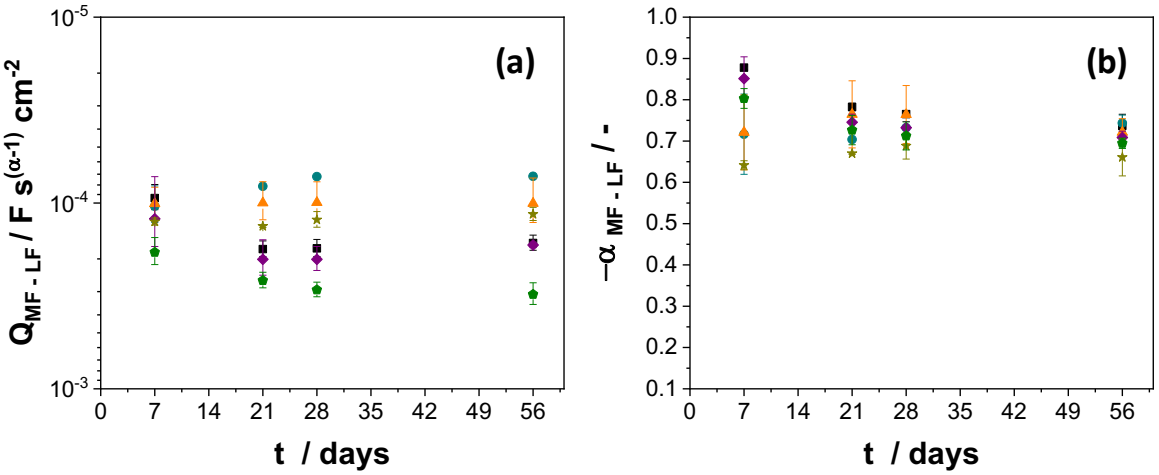

Figure 12: Variation of CPE parameters of reinforcement mortars at low-frequency range in $Ca(OH)_{2,sat}$ at 23 °C and E=E_{oc}. (■) 0 wt. %, (●) 15 wt. %, (▲) 20 wt. %, (♦) 25 wt. %, (★) 30 wt. % & (⬟) wt. 50%.

Liao et al. proposed that the impedance response at frequency approaches zero, and the modulus at low frequency (LF) can be related to the polarization resistance (R_p) (Liao et al., 2020; Sancy et al., 2010). Note that the polarization resistance can be defined as the metal's ability to resist oxidation when an external potential is applied. In addition, the corrosion rate is directly linked to the polarization resistance, suggesting that a higher polarization resistance indicates a reduced corrosion rate(Toshev et al., 2006). Figure 12 shows the evolution of the impedance modulus at low frequency ($|Z|_{LF}$) obtained by adjusting (Orazem & Tribollet, 2017), revealing that the sample with 15 wt. % of cement replacement increased over time, possibly due to the growth of a physical barrier against corrosion attack. Cement replacement over 25 wt.% reduced the bar protection, with a behavior similar to the control sample. Nonetheless, the $|Z|_{LF}$ increased slightly in almost all the samples by incorporating copper tailings.

Figure 13 shows the linear sweep voltammetry of reinforced mortar samples after 56 days of exposure, revealing that the corrosion potential (E_{corr}) was slightly shifted towards more positive values with the 15 wt. % cement replacement by copper tailings, in agreement with the evolution of E_{oc}. In addition, a reduction in the current density (I_{corr}) was observed using 15 wt.% as cement replacement, suggesting a decrease in the corrosion resistance, in agreement with the impedance analysis.

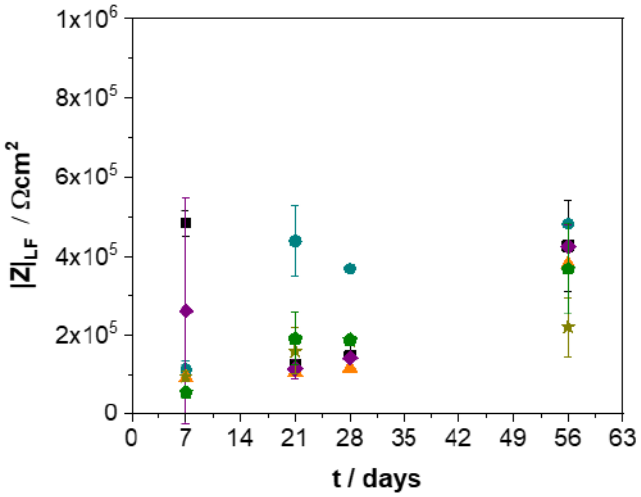

Figure 12. Effect of cement replacement on the impedance module of reinforced mortars at low frequency at 23 °C and E=E_{oc}. (■) 0 wt. %, (●) 15 wt. %, (▲) 20 wt. %, (♦) 25 wt. %, (★) 30 wt. % & (⬟) wt. 50%.

4. Conclusion

The effect of copper tailing on the mechanical and electrochemical properties of mortar and reinforced mortar was analyzed, which allowed us to conclude that incorporating copper tailings, as received, could improve the pozzolanic capacity, with a critical cement replacement between 0 to 20 wt. %.

(1) The increase in porosity affects the mechanical response, determined when the copper tailing was incorporated over 15 wt.%. Therefore, it is essential to consider the water/cement ratio when copper tailing is used as cement replacement since it can increase the porosity even more.

(2) Incorporating copper tailing in critical content can favor the passivation of steel bars due to decreased percolating pores.

(3) Impedance analysis is a valuable technique to monitor in situ porosity and passivation evolution for reinforced concrete structures.

Acknowledgments

The authors would like to thank: France-Chile ECOS (Grant C17E0), ANID PFCHA/Doctorado Becas Chile/2019 (Grant 21190220) and Postdoctoral N°3210432, Fondequip (EQM 160091 and 150101), and Millennium Institute on Green Ammonia (Grant ICN2021_023).

5. References

A study on mechanical properties and permeability of steam-cured mortar with iron-copper tailings. (n.d.).

Andrade, C., Keddam, M., Nóvoa, X. R., Pérez, M. C., Rangel, C. M., & Takenouti, H. (2001). Electrochemical behaviour of steel rebars in concrete: Influence of environmental factors and cement chemistry. *Electrochimica Acta*, *46*(24–25), 3905–3912. https://doi.org/10.1016/S0013-4686(01)00678-8

Andrade, C., Soler, L., & Novoa, X. R. (1995). Advances in electrochemical impedance measurements in reinforced concrete. *Materials Science Forum*, *192–194*(pt 2), 843–856. https://doi.org/10.4028/www.scientific.net/msf.192-194.843

ASTM International. (2015). Standard test method for corrosion potentials of uncoated reinforcing steel in concrete. ASTM C876 - 15. G01.14,. *ASTM International*, 1–8. https://doi.org/10.1520/C0876-15.2

Ayati, B., Newport, D., Wong, H., & Cheeseman, C. (2022). Low-carbon cements: Potential for low-grade calcined clays to form supplementary cementitious materials. *Cleaner Materials*, *5*, 100099. https://doi.org/10.1016/j.clema.2022.100099

Bentz, D. P., Jensen, O. M., Coats, A. M., & Glasser, F. P. (n.d.). *Influence of silica fume on diffusivity in cement-based materials I. Experimental and computer modeling studies on cement pastes*.

Cao, Z., Shen, L., Zhao, J., Liu, L., Zhong, S., Sun, Y., & Yang, Y. (2016). Toward a better practice for estimating the CO2 emission factors of cement production: An experience from China. *Journal of Cleaner Production*, *139*, 527–539. https://doi.org/10.1016/j.jclepro.2016.08.070

Dandautiya, R., & Singh, A. P. (2019). Utilization potential of fly ash and copper tailings in concrete as partial replacement of cement along with life cycle assessment. *Waste Management*, *99*, 90–101. https://doi.org/10.1016/J.WASMAN.2019.08.036

Esmaeili, J., & Aslani, H. (2019a). Use of copper mine tailing in concrete: strength characteristics and durability performance. *Journal of Material Cycles and Waste Management*, *21*(3), 729–741. https://doi.org/10.1007/s10163-019-00831-7

Esmaeili, J., & Aslani, H. (2019b). Use of copper mine tailing in concrete: strength characteristics and durability performance. *Journal of Material Cycles and Waste Management*, *21*, 729–741. https://doi.org/10.1007/s10163-019-00831-7

Esmaeili, J., Aslani, H., & Onuaguluchi, O. (2020). Reuse Potentials of Copper Mine Tailings in Mortar and Concrete Composites. *Journal of Materials in Civil Engineering*, *32*(5), 04020084. https://doi.org/10.1061/(ASCE)MT.1943-5533.0003145

Gharbi, O., Dizon, A., Orazem, M. E., Tran, M. T. T., Tribollet, B., & Vivier, V. (2019). From frequency dispersion to ohmic impedance: A new insight on the high-frequency impedance analysis of electrochemical systems. *Electrochimica Acta*, *320*. https://doi.org/10.1016/j.electacta.2019.134609

Gonzalez, J. A., Molina, A., Escudero, M. L., & Andradet, C. (1985). ERRORS IN THE ELECTROCHEMICAL EVALUATION OF VERY SMALL CORROSION RATES-I. POLARIZATION RESISTANCE METHOD APPLIED TO CORROSION OF STEEL IN CONCRETE. In *Corrosion Science* (Vol. 25, Issue 10).

Güneyisi, E., Gesoğlu, M., Karaoğlu, S., & Mermerdaş, K. (2012). Strength, permeability and shrinkage cracking of silica fume and metakaolin concretes. *Construction and Building Materials*, *34*, 120–130. https://doi.org/10.1016/j.conbuildmat.2012.02.017

Hasanbeigi, A., Price, L., & Lin, E. (2012a). Emerging energy-efficiency and CO 2 emission-reduction technologies for cement and concrete production: A technical review. In *Renewable and Sustainable Energy Reviews* (Vol. 16, Issue 8, pp. 6220–6238). Pergamon. https://doi.org/10.1016/j.rser.2012.07.019

Hasanbeigi, A., Price, L., & Lin, E. (2012b). Emerging energy-efficiency and CO 2 emission-reduction technologies for cement and concrete production: A technical review. In *Renewable and Sustainable Energy Reviews* (Vol. 16, Issue 8, pp. 6220–6238). https://doi.org/10.1016/j.rser.2012.07.019

Hemkemeier, T. A., Almeida, F. C. R., Sales, A., & Klemm, A. J. (2022). Corrosion monitoring by open circuit potential in steel reinforcements embedded in cementitious composites with industrial wastes. *Case Studies in Construction Materials*, *16*. https://doi.org/10.1016/j.cscm.2022.e01042

Hossain, M. U., Poon, C. S., Dong, Y. H., & Xuan, D. (2018). Evaluation of environmental impact distribution methods for supplementary cementitious materials. In *Renewable and Sustainable Energy Reviews* (Vol. 82, pp. 597–608). Elsevier Ltd. https://doi.org/10.1016/j.rser.2017.09.048

Imbabi, M. S., Carrigan, C., & McKenna, S. (2012). Trends and developments in green cement and concrete technology. *International Journal of Sustainable Built Environment*, *1*(2), 194–216. https://doi.org/10.1016/j.ijsbe.2013.05.001

Jorcin, J. B., Orazem, M. E., Pébère, N., & Tribollet, B. (2006). CPE analysis by local electrochemical impedance spectroscopy. *Electrochimica Acta*, *51*(8–9), 1473–1479. https://doi.org/10.1016/j.electacta.2005.02.128

Juenger, M. C. G., & Siddique, R. (2015). Recent advances in understanding the role of supplementary cementitious materials in concrete. *Cement and Concrete Research*, *78*, 71–80. https://doi.org/10.1016/j.cemconres.2015.03.018

Juenger, M. C. G., Snellings, R., & Bernal, S. A. (2019). Supplementary cementitious materials: New sources, characterization, and performance insights. *Cement and Concrete Research*, *122*(February), 257–273. https://doi.org/10.1016/j.cemconres.2019.05.008

Kajaste, R., & Hurme, M. (2016). Cement industry greenhouse gas emissions - Management options and abatement cost. *Journal of Cleaner Production*, *112*, 4041–4052. https://doi.org/10.1016/j.jclepro.2015.07.055

Lehne, J., & Preston, F. (2018). *Making Concrete Change Innovation in Low-carbon Cement and Concrete The Royal Institute of International Affairs, Chatham House Report Series, www.chathamhouse.org/sites/default/files/publications/research/2018-06-13-makingconcrete- c*. 138. www.chathamhouse.org

Liao, H., Watson, W., Dizon, A., Tribollet, B., Vivier, V., & Orazem, M. E. (2020). Physical properties obtained from measurement model analysis of impedance measurements. *Electrochimica Acta*, *354*. https://doi.org/10.1016/j.electacta.2020.136747

Liu, G., Zhang, Y., Wu, M., & Huang, R. (2017). Study of depassivation of carbon steel in simulated concrete pore solution using different equivalent circuits. *Construction and Building Materials*, *157*, 357–362. https://doi.org/10.1016/j.conbuildmat.2017.09.104

Lothenbach, B., Bernard, E., & Mäder, U. (2017). Zeolite formation in the presence of cement hydrates and albite. *Physics and Chemistry of the Earth*, *99*, 77–94. https://doi.org/10.1016/j.pce.2017.02.006

Mabroum, S., Moukannaa, S., El Machi, A., Taha, Y., Benzaazoua, M., & Hakkou, R. (2020). Mine wastes based geopolymers: A critical review. In *Cleaner Engineering and Technology* (Vol. 1). Elsevier Ltd. https://doi.org/10.1016/j.clet.2020.100014

Medina, J. M., de Rojas, M. I. S., Sáez Del Bosque, I. F., Frías, M., & Medina, C. (2020). Sulfate resistance in cements bearing bottom ash from biomass-fired electric power plants. *Applied Sciences (Switzerland)*, *10*(24), 1–11. https://doi.org/10.3390/app10248982

Mehenni, A., Cuisinier, O., & Masrouri, F. (2016). Impact of Lime, Cement, and Clay Treatments on the Internal Erosion of Compacted Soils. *Journal of Materials in Civil Engineering*, *28*(9), 04016071. https://doi.org/10.1061/(asce)mt.1943-5533.0001573

Navarrete, I., Kurama, Y., Escalona, N., Brevis, W., & Lopez, M. (2022). Effect of supplementary cementitious materials on viscosity of cement-based pastes. *Cement and Concrete Research*, *151*. https://doi.org/10.1016/j.cemconres.2021.106635

Nóvoa, X. R. (2016). Electrochemical aspects of the steel-concrete system. A review. *Journal of Solid State Electrochemistry*, *20*(8), 2113–2125. https://doi.org/10.1007/s10008-016-3238-z

Onuaguluchi, O., & Eren, Ö. (2012a). Copper tailings as a potential additive in concrete: consistency, strength and toxic metal immobilization properties. In *Indian Journal of Engineering & Materials Sciences* (Vol. 19).

Onuaguluchi, O., & Eren, Ö. (2012b). Rheology, strength and durability properties of mortars containing copper tailings as a cement replacement material Rheology, strength and durability properties of mortars containing copper tailings as a cement replacement material. *European Journal of Environmental and Civil Engineering* . https://doi.org/10.1080/19648189.2012.699708

Orazem, M. E., & Tribollet, B. (2017). Graphical Methods. In *Electrochemical Impedance Spectroscopy* (pp. 493–526). John Wiley & Sons, Inc. https://doi.org/10.1002/9781119363682.ch18

Pacheco Torgal, F., Miraldo, S., Labrincha, J. A., & De Brito, J. (2012). *An overview on concrete carbonation in the context of eco-efficient construction: Evaluation, use of SCMs and/or RAC*. https://doi.org/10.1016/j.conbuildmat.2012.04.066

Petersson, I., Lilja, M., Hammel, J., & Kottorp, A. (2008). Impact of home modification services on ability in everyday life for people ageing with disabilities. *Journal of Rehabilitation Medicine*, *40*(4), 253–260. https://doi.org/10.2340/16501977-0160

Pokorný, J., Pavlíková, M., Záleská, M., Rovnaníková, P., & Pavlík, Z. (2016). Coagulated silica - A-SiO2 admixture in cement paste. *AIP Conference Proceedings*, *1752*. https://doi.org/10.1063/1.4955254

Qing, L., Shaokang, S., Zhen, J., Junxiang, W., & Xianjun, L. (2021). Effect of CaO on hydration properties of one-part alkali-activated material prepared from tailings through alkaline hydrothermal activation. *Construction and Building Materials*, *308*. https://doi.org/10.1016/j.conbuildmat.2021.124931

Sánchez de Rojas, M. I., Rivera, J., Frías, M., & Marín, F. (2008). Use of recycled copper slag for blended cements. In *Journal of Chemical Technology and Biotechnology* (Vol. 83, Issue 3, pp. 209–217). https://doi.org/10.1002/jctb.1830

Sancy, M., Gourbeyre, Y., Sutter, E. M. M., & Tribollet, B. (2010). Mechanism of corrosion of cast iron covered by aged corrosion products: Application of electrochemical impedance spectrometry. *Corrosion Science*, *52*(4), 1222–1227. https://doi.org/10.1016/j.corsci.2009.12.026

Smuda, J., Dold, B., Spangenberg, J. E., Friese, K., Kobek, M. R., Bustos, C. A., & Pfeifer, H. R. (2014). Element cycling during the transition from alkaline to acidic environment in an active porphyry copper tailings impoundment, Chuquicamata, Chile. *Journal of Geochemical Exploration*, *140*, 23–40. https://doi.org/10.1016/j.gexplo.2014.01.013

Smuda, J., Dold, B., Spangenberg, J. E., & Pfeifer, H. R. (2008). Geochemistry and stable isotope composition of fresh alkaline porphyry copper tailings: Implications on sources and mobility of elements during transport and early stages of deposition. *Chemical Geology*, *256*(1–2), 62–76. https://doi.org/10.1016/j.chemgeo.2008.08.001

Stefanoni, M., Angst, U., & Elsener, B. (2018). Corrosion rate of carbon steel in carbonated concrete – A critical review. In *Cement and Concrete Research* (Vol. 103, pp. 35–48). Elsevier Ltd. https://doi.org/10.1016/j.cemconres.2017.10.007

Sun, X., Liu, J., Zhao, Y., Zhao, J., Li, Z., Sun, Y., Qiu, J., & Zheng, P. (2022). Mechanical activation of steel slag to prepare supplementary cementitious materials: A comparative research based on the particle size distribution, hydration, toxicity assessment and carbon dioxide emission. *Journal of Building Engineering*, *60*. https://doi.org/10.1016/j.jobe.2022.105200

Toshev, Y., Mandova, V., Boshkov, N., Stoychev, D., Petrov, P., Tsvetkova, N., Raichevski, G., Tsvetanov, C., Gabev, A., Velev, R., & Kostadinov, K. (2006). *Protective coating of zinc and zinc alloys for industrial applications*.

Vargas, F., & Lopez, M. (2018). Development of a new supplementary cementitious material from the activation of copper tailings: Mechanical performance and analysis of factors. *Journal of Cleaner Production*, *182*, 427–436. https://doi.org/10.1016/j.jclepro.2018.01.223

Vargas, F., Lopez, M., & Rigamonti, L. (2020). Environmental impacts evaluation of treated copper tailings as supplementary cementitious materials. *Resources, Conservation and Recycling*, *160*. https://doi.org/10.1016/j.resconrec.2020.104890

Wang, Y., Zhao, C., Chen, P., Wang, C., Tan, W., Qian, X., & Qiao, X. (2023). Preparation of mortars using bio-functionalized copper tailings. *Journal of Building Engineering*, *77*. https://doi.org/10.1016/j.jobe.2023.107460

You, N., Shi, J., & Zhang, Y. (2022). Electrochemical performance of low-alloy steel and low-carbon steel immersed in the simulated pore solutions of alkali-activated slag/steel slag pastes in the presence of chlorides. *Corrosion Science*, *205*. https://doi.org/10.1016/j.corsci.2022.110438

Zhang, L., Li, J., & Qiao, H. (2019). Effect of copper tailing content on corrosion resistance of steel reinforcement in a Salt Lake environment. *Materials*, *12*(19). https://doi.org/10.3390/MA12193069

5. Supplementary Materials

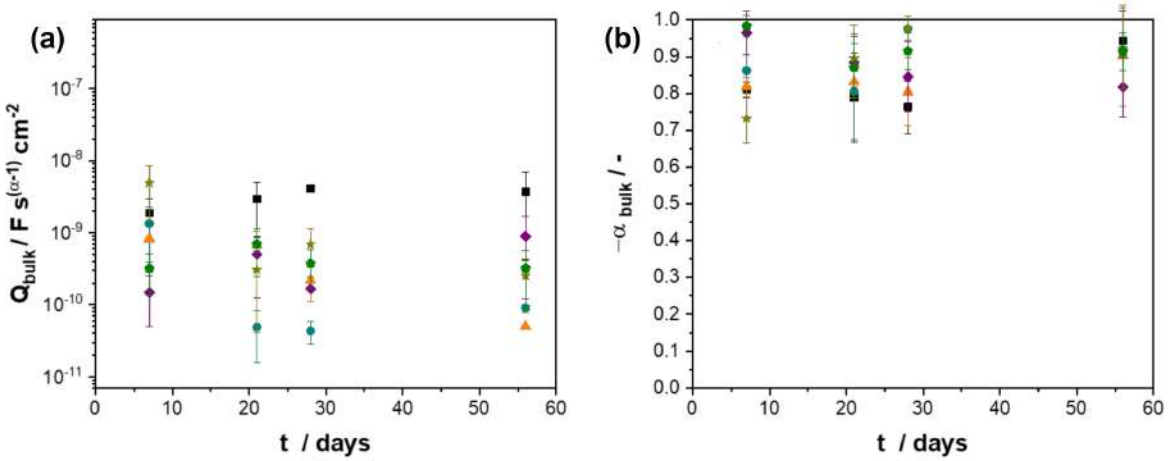

Figure S1: Variation of CPE parameters of reinforcement mortars of bulk part of mortars in $Ca(OH)_{2,sat}$ at T_{amb} and E=E_{oc}. (■) 0 wt. %, (●) 15 wt. %, (▲) 20 wt. %, (♦) 25 wt. %, (★) 30 wt. % & (⬟) wt. 50%.